

# PICOMETER-SCALE EMITTANCE AND SPACE CHARGE EFFECTS IN NANOSTRUCTURED PHOTOCATHODES

A. Ullattuparambil\*, M. M. Rizi, P. P. Owusu, S. Karkare

Arizona State University, Tempe, AZ, USA

M. Kaemingk, Los Alamos National Laboratory, Los Alamos, NM, USA

A. Bartnik, M. Gordon, C. Abbamonte, S. Levenson, J. Maxson

Cornell University, Ithaca, NY, USA

## Abstract

Generation of ultra-low emittance electron beams with high brightness is critical for several applications such as ultrafast electron diffraction, microscopy, and advanced accelerator techniques. By leveraging the differences in work function and electronic structure between different materials, we enabled spatially localized photoemission, resulting in picometer-scale emittance from a flat photocathode. We also investigated space charge effects by measuring how the emission spot size, as measured in a photoemission electron microscope, changes with the number of electrons emitted per laser pulse. When more than one electron is emitted simultaneously, Coulomb repulsion causes a substantial broadening of the observed source size, enabling us to investigate the limitations imposed by vacuum space charge forces during pulsed photoemission. Our results highlight the potential of nanoscale photoemitters as high-brightness electron sources and offer new insights into electron correlations that emerge after ultra-fast photoemission.

## INTRODUCTION

Femtosecond-scale pulsed electron sources are indispensable for probing atomic motion with sub-ångström spatial resolution in ultrafast electron diffraction and microscopy (UED/UEM) [1–4]. The normalized transverse emittance sets the fundamental limit on the attainable spatial resolution in these applications, motivating ongoing efforts to achieve picometer-level emittance directly at the photocathode. Although field-emission cathodes can deliver sub-picometer emittance, they operate in continuous mode and suffer from poor survivability under the high electric fields of modern accelerator structures. Consequently, photoemission remains the most viable approach for generating high-brightness, ultrafast electron pulses compatible with high-field accelerator environments.

The normalized transverse emittance of an electron bunch is given by [5]:

$$\epsilon_{n,x} = \sigma_x \sqrt{\frac{\text{MTE}}{m_e c^2}} \quad (1)$$

where  $\sigma_x$  is the root-mean-square (RMS) emission area and MTE is the mean transverse energy of the emitted electrons. This expression illustrates that the emittance can be

reduced by minimizing either the MTE or the emission spot size.

The MTE reflects the transverse momentum spread of the photoemitted electrons and is mainly determined by the photocathode material, its band structure, physical and chemical roughness, and the photon energy of excitation light. According to the Dowell-Schmerge model, the MTE of emitted electrons varies linearly with the excess energy, that is, the difference between the photon energy and the material's work function [6]—and approaches the thermal limit as the photon energy approaches the work function [7]. Atomically ordered surfaces have demonstrated ultra-low mean transverse energies (MTEs), further minimized by operation near the photoemission threshold at low temperatures [8].

For applications like stroboscopic UED/UEM where single to few electrons per bunch are sufficient, the smallest possible emission area is typically governed by the smallest possible laser spot size, which is restricted to the few micrometer scale due to the diffraction limit of light. Reducing this size below the diffraction limit of light requires alternative strategies to produce sub-micron-sized electron beams.

Recent advancements include nano-localized linear photoemission from a Schottky emitter, which enabled transverse emittances as low as 13.25 pm·rad [9]. Nonetheless, these emitters face limitations such as reduced operational lifetime at high electric fields and undesirable dark current due to field emission, making them unsuitable for RF gun environments. Other efforts have employed plasmonic interference to confine emission, achieving a record emittance of 40 pm·rad from flat photocathodes via nonlinear photoemission using circularly polarized light [10]. However, the higher MTE and energy spread associated with nonlinear emission limit the achievable emittance [11].

In this work, we demonstrate a novel photocathode concept that simultaneously addresses both MTE and emission area reduction using a geometrically flat photocathode, as shown in Fig 1. By patterning a circular region of low work function material on a high work function background, and by operating the photocathode at a photon energy between the two work functions, we spatially confine the photoemission to a sub-um scale area while maintaining low MTE. We achieved a low rms emission area of 106 nm from a gold photocathode fabricated on Silicon. Additionally, we demonstrate spatially confined photoemission from a metal-on-metal photocathode comprising platinum dots patterned

\* aullattu@asu.edu

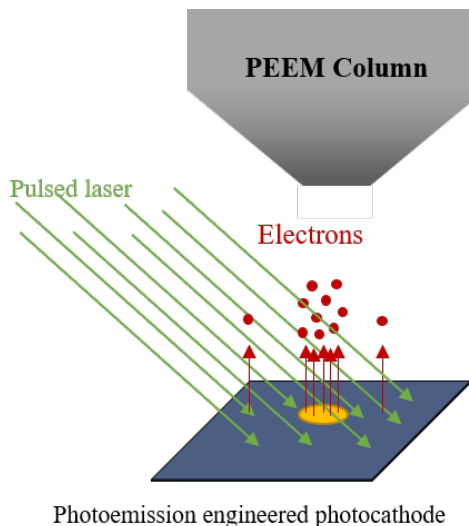


Figure 1: Schematic of a photoemission-engineered photocathode illuminated by a laser with photon energy between the work functions of two materials. Significant photoemission occurs only from the region with the lower work function, while emission from the higher work function region is suppressed.

on a copper film. We further investigate the space charge effects that arise during pulsed photoemission from such nano-engineered cathodes and evaluate the corresponding limits imposed on beam brightness.

## EXPERIMENTAL DETAILS

Circular gold dots with diameters ranging from 10  $\mu\text{m}$  to 150 nm were fabricated on a silicon substrate using electron beam lithography [10]. The Pt dots on Cu were fabricated using photolithography, and dots as small as 500 nm were produced. The samples were transferred into a commercially available photoemission electron microscope (PEEM) [12] after an ultrahigh vacuum (UHV) bake-out at 110–130 °C for two days. Photoemission characterization was performed using both a 240 nm continuous-wave mercury lamp and a femtosecond pulsed laser (150 fs pulse duration, 500 kHz repetition rate) at UV wavelengths. The laser was made incident onto the sample at 65 degree angle of incidence, and was focused down to a spot size of 100  $\mu\text{m}$  full width at half maximum (FWHM) at the photocathode surface. Emission from both the gold and silicon regions was analyzed. The emission confinement, photocurrent, mean transverse energy (MTE), and electron energy distribution were measured using the PEEM.

## RESULTS AND DISCUSSION

### Emission Confinement

The work functions of Gold and Si were obtained to be 3.76 eV and 4.36 eV, respectively, using the energy distributions measured in the PEEM [13]. The substantially lower measured work function of gold, as compared to its theo-

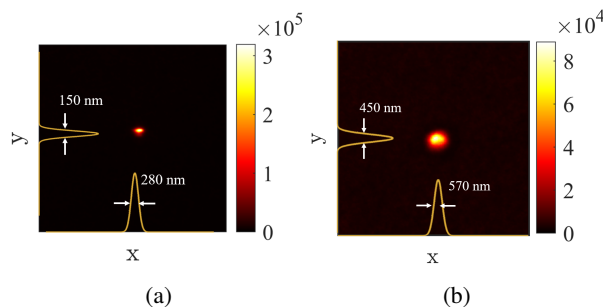


Figure 2: (a) Photoemission electron microscopy (PEEM) image of 150 nm diameter gold dot acquired at a photon energy of 4.28 eV. (b) PEEM image of a 500 nm platinum dot on Copper, operated using uniform illumination with continuous wave 5.16 eV Mercury lamp. The color bar indicates the photoemission intensity in arbitrary units as measured by the PEEM.

retical value, has been attributed to the presence of organic contaminants on the surface [14]. The pronounced difference in work functions between the gold dot and the surrounding substrate results in spatially confined photoemission from the gold. This confinement persists for photon energies that lie between the work functions of the two materials, effectively suppressing emission from the silicon while enabling efficient emission from the gold region. A similar work function contrast between platinum and copper facilitated spatially localized photoemission from a metal-on-metal photocathode. Such a metal-on-metal system will be significantly easier to use in an RF gun. Figures 2(a) and 2(b) show PEEM images of a 150 nm gold dot and a 500 nm platinum dot, respectively, each operated at photon energies lying between the work functions of the photoemitter and the substrate.

To quantify the degree of photoemission contrast, we calculated the extinction ratio, defined as the ratio of the quantum efficiency (QE) of the substrate to that of the photoemitting region, across various photon energies for both photocathode systems. Extinction ratios as low as  $1 \times 10^{-7}$  for the gold-on-silicon system and  $1 \times 10^{-5}$  for the platinum-on-copper system were achieved. These exceptionally low values indicate strong suppression of photoemission from the surrounding substrate, confirming the high contrast and confinement achieved in both designs.

### MTE and Emittance

As the photocathode is operated at photon energies near the work function of gold, the emitted electrons exhibit a low mean transverse energy (MTE), consistently below 100 meV across all measured gold dots. At these near-threshold energies, thermal excitation is minimized, resulting in reduced excess energy and therefore lower transverse momentum spread. The root-mean-square (RMS) emission spot size, MTE, and the corresponding normalized transverse emittance values are summarized in Table 1. Notably, we achieved an exceptionally low normalized emittance of 36.25

Table 1: Dependence of MTE and Transverse Emittance on Dot Diameter for Gold on P-Type Silicon Photocathode

Dot Diameter	Emission Size RMS	MTE (meV)	Emittance (pm.rad)
10 $\mu\text{m}$	3.231 $\mu\text{m}$	138	1675.51
5 $\mu\text{m}$	1.565 $\mu\text{m}$	153	854.73
2 $\mu\text{m}$	616 nm	94	263.52
1 $\mu\text{m}$	316 nm	164	178.87
500 nm	194 nm	142	102.26
200 nm	125 nm	91	52.72
150 nm	106 nm	60	36.25

pm.rad from the 150 nm diameter gold dot, demonstrating the effectiveness of size confinement and threshold operation in minimizing emittance for photoemission electron sources.

A variation in MTE was also observed across different gold dots. This trend may be attributed to chemical roughness at the gold–silicon interface, arising from the significant work function difference between the two materials [15]. A more detailed investigation of these interface-induced electronic effects is a subject of our ongoing work.

### Electron-Electron Interactions

Space charge effects impose a fundamental limitation on beam brightness by causing emittance degradation at high emission currents, due to Coulomb repulsion between electrons [16, 17]. In the context of pulsed photoemission, these effects are strongly governed by several source parameters, including the number of electrons per pulse, the laser spot size on the photocathode, and the pulse duration. A significant increase in the emission spot size, as measured by PEEM, was observed for all dots once the average number of emitted electrons per pulse exceeded one, despite maintaining a constant incident laser spot size. Figure 3 illustrates the increase in both the size of the PEEM image and the number of electrons emitted per pulse from a 500 nm dot of Au on Si at a photon energy of 4.59 eV, as a function of peak laser pulse power. The PEEM images of the 500 nm dot at two different laser powers, highlighting the corresponding change in photoemission behavior, are shown in Fig. 4. Our results show that the electron-electron Coulomb effects can be easily detected even in the presence of only two electrons per shot, making such nanoscale emission areas an excellent system to experimentally study and engineer coulomb effects between individual electrons.

## CONCLUSION

By harnessing the difference in work function and electronic properties of two materials, we achieved spatially confined photoemission from gold-on-silicon, and platinum-on-copper photocathodes. This approach was further advanced to enable patterned electron emission from a high-quantum-efficiency cesium antimonide ( $\text{Cs}_3\text{Sb}$ ) photocathode under visible-light illumination. This strategy enables controlled spatial emission by engineering local work function land-

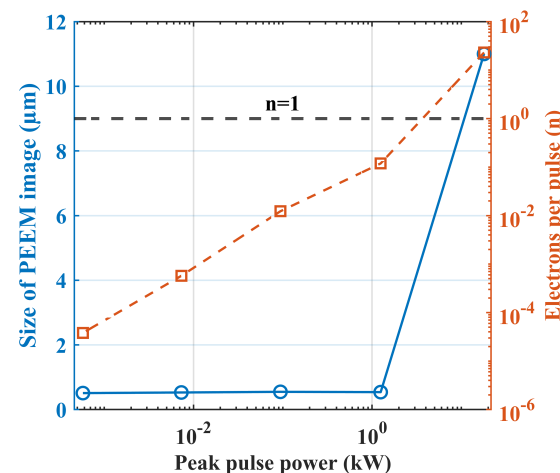


Figure 3: Size of the PEEM image of a 500 nm gold dot, and the number of electrons per pulse from a same dot as a function of peak laser pulse power. The left axis (blue) shows the emission spot size as measured in the PEEM, which remains nearly constant - 500 nm - at low pulse powers. The right axis (orange) plots the number of emitted electrons per pulse on a logarithmic scale, showing a linear increase with pulse power. The dashed line at  $n=1$  marks the one electron per pulse threshold, above which space-charge effects may become significant, and results in a substantial increase in emission area as measured in the PEEM.

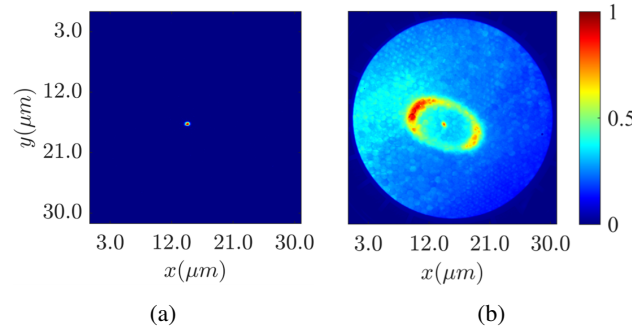


Figure 4: Image of 500 nm diameter dot taken at two different laser power using PEEM, demonstrating significant increase in the size of the PEEM image measured at higher laser power: (a) Low laser power, yielding  $3.82 \times 10^{-5}$  electrons per pulse, (b) Higher laser power, yielding 11 electrons per pulse. The color bar indicates the photoemission intensity scaled to max 1 for both images.

scapes across the emitter surface. In addition, to investigate the impact of space charge on emission characteristics of nanoscale electron sources, we analyzed the broadening of the emission spot as a function of emitted charge. Our observations revealed a significant increase in the apparent source size when more than one electron was emitted per pulse, providing direct evidence of space-charge-induced emittance degradation at the source. These findings highlight the intrinsic limitations imposed by space charge in ultrafast photoemission processes from nanoscale emission sites.

## ACKNOWLEDGEMENTS

This work was supported by the U.S. National Science Foundation under Award No. PHY1549132 the Center for Bright Beams, U.S. Department of Energy, Grant No. DE-SC0021092, DE-SC0020575, DE-SC0020144, and DE-SC0024845.

## REFERENCES

- [1] D. Durham *et al.*, “Relativistic ultrafast electron diffraction of nanomaterials”, *Microsc. Microanal.*, vol. 26, no. S2, pp. 676–677, 2020. doi:10.1017/S1431927620015494
- [2] F. Ji, D. B. Durham, A. M. Minor, P. Musumeci, J. G. Navarro, and D. Filippetto, “Ultrafast relativistic electron nanoprobe”, *Commun. Phys.*, vol. 2, no. 1, pp. 1–10, 2019. doi:10.1038/s42005-019-0154-4
- [3] A. H. Zewail, “4d ultrafast electron diffraction, crystallography, and microscopy”, *Annu. Rev. Phys. Chem.*, vol. 57, no. 1, pp. 65–103, 2006. doi:10.1146/annurev.physchem.57.032905.104748
- [4] C. Kisielowski *et al.*, “Detection of single atoms and buried defects in three dimensions by aberration-corrected electron microscope with 0.5- $\text{\AA}$  information limit”, *Microsc. Microanal.*, vol. 14, no. 5, pp. 469–477, 2008. doi:10.1017/S1431927608080902
- [5] S. Karkare *et al.*, “Ultrabright and ultrafast III–v semiconductor photocathodes”, *Phys. Rev. Lett.*, vol. 112, no. 9, p. 097601, 2014. doi:10.1103/PhysRevLett.112.097601
- [6] D. H. Dowell and J. F. Schmerge, “Quantum efficiency and thermal emittance of metal photocathodes”, *Phys. Rev. Spec. Top. Accel. Beams*, vol. 12, no. 7, p. 074201, 2009. doi:10.1103/PhysRevSTAB.12.074201
- [7] J. Feng, J. Nasiatka, W. Wan, S. Karkare, J. Smedley, and H. A. Padmore, “Thermal limit to the intrinsic emittance from metal photocathodes”, *Appl. Phys. Lett.*, vol. 107, no. 13, p. 134101, 2015. doi:10.1063/1.4931976
- [8] S. Karkare *et al.*, “Ultracold electrons via near-threshold photoemission from single-crystal cu(100)”, *Phys. Rev. Lett.*, vol. 125, no. 5, p. 054801, 2020. doi:10.1103/PhysRevLett.125.054801
- [9] A. Feist *et al.*, “Ultrafast transmission electron microscopy using a laser-driven field emitter: Femtosecond resolution with a high coherence electron beam”, *Ultramicroscopy*, vol. 176, pp. 63–73, 2017. doi:10.1016/j.ultramic.2016.12.005
- [10] A. Kachwala, M. M. Rizi, C. M. Pierce, D. Filippetto, J. Maxson, and S. Karkare, “Harnessing plasmonic interference for nanoscale ultrafast electron sources”, *Phys. Rev. Lett.*, vol. 133, no. 18, p. 185001, 2024. doi:10.1103/PhysRevLett.133.185001
- [11] C. J. Knill *et al.*, “Effects of nonlinear photoemission on mean transverse energy from metal photocathodes”, *Phys. Rev. Accel. Beams*, vol. 26, no. 9, p. 093401, 2023. doi:10.1103/PhysRevAccelBeams.26.093401
- [12] “PEEM | FOCUS - instruments for electron spectroscopy and surface analysis”, <https://www.focus-gmbh.com/peem-nanoesca/peem/>
- [13] A. Kachwala, P. Saha, P. Bhattacharyya, E. Montgomery, O. Chubenko, and S. Karkare, “Demonstration of thermal limit mean transverse energy from cesium antimonide photocathodes”, *Appl. Phys. Lett.*, vol. 123, no. 4, p. 044106, 2023. doi:10.1063/5.0159924
- [14] B. Aghili, S. Rahbarpour, M. Berahman, and A. Horri, “Influence of surface roughness on the work function of gold: A density functional theory study”, *J. Phys. Chem. C*, vol. 128, no. 19, pp. 8077–8084, 2024. doi:10.1021/acs.jpcc.4c01068
- [15] G. S. Gevorkyan, S. Karkare, S. Emamian, I. V. Bazarov, and H. A. Padmore, “Effects of physical and chemical surface roughness on the brightness of electron beams from photocathodes”, *Phys. Rev. Accel. Beams*, vol. 21, no. 9, p. 093401, 2018. doi:10.1103/PhysRevAccelBeams.21.093401
- [16] J. Graf *et al.*, “Vacuum space charge effect in laser-based solid-state photoemission spectroscopy”, *J. Appl. Phys.*, vol. 107, no. 1, p. 014912, 2010. doi:10.1063/1.3273487
- [17] S. Hellmann, K. Rossnagel, M. Marczynski-Bühlow, and L. Kipp, “Vacuum space-charge effects in solid-state photoemission”, *Phys. Rev. B*, vol. 79, no. 3, p. 035402, 2009. doi:10.1103/PhysRevB.79.035402